

A Parallel Numerical Method to Solve High Frequency Ghost Obstacle Acoustic Scattering Problems

¹L. Fatone, ²M. C. Recchioni, and ³F. Zirilli

¹ Dipartimento di Matematica Pura e Applicata, University of Modena e Reggio Emilia, Modena, Italy

² Dipartimento di Scienze Sociali "D. Serrani", University Politecnica delle Marche, Ancona, Italy

³ Dipartimento di Matematica "G. Castelnuovo", University of Roma "La Sapienza", Roma, Italy

Abstract – A highly parallelizable numerical method for time dependent high frequency acoustic scattering problems involving realistic smart obstacles is proposed. A scatterer becomes smart when hit by an incoming wave reacts circulating on its boundary a pressure current to pursue a given goal. A pressure current is a quantity whose physical dimension is pressure divided by time. In particular in this paper we consider obstacles that when hit by an incoming acoustic wave try to generate a virtual image of themselves in a location in space different from their actual location. The virtual image of the obstacle (i.e.: the ghost obstacle) is seen outside a given set containing the obstacle and its virtual image in the apparent location. We call this problem ghost obstacle scattering problem. We model this acoustic scattering problem and several other acoustic scattering problems concerning other types of smart obstacles as optimal control problems for the wave equation. Using the Pontryagin maximum principle the first order optimality conditions associated to these control problems are formulated. The numerical method proposed to solve these optimality conditions is a variation of the operator expansion method and reduces the solution of the optimal control problem to the solution of a sequence of systems of integral equations. These systems of integral equations are solved using suitable wavelet bases to represent the unknowns, the data and the integral kernels. These wavelet bases are made of piecewise polynomial functions and have the property that the matrices that represent the integral operators on these wavelet bases can be approximated satisfactorily with very sparse matrices. This property of the wavelet bases makes possible to approximate the optimal control problems considered with linear systems of equations with hundreds of thousands or millions of unknowns and equations that can be stored and solved with affordable computing resources, that is it makes possible to solve satisfactorily problems with realistic obstacles hit by waves of small wavelength. We validate the method proposed solving some test problems, these problems are optimal control problems involving a "smart" simplified version of the NASA space shuttle hit by incoming waves with small wavelengths compared to its characteristic dimension. We consider test problems with ratio between the characteristic dimension of the obstacle and the wavelength of the time harmonic component of the incoming wave up to approximately sixty. The numer-

ical results obtained are very satisfactory. The website: <http://www.econ.univpm.it/recchioni/scattering/w16> contains stereographic and virtual reality applications showing some numerical experiments relative to the problems studied in this paper. A more general reference to the work in acoustic and electromagnetic scattering of the authors and of their coauthors is the website: <http://www.econ.univpm.it/recchioni/scattering>.

Keywords: Acoustic obstacle scattering, smart obstacles, open loop control, operator expansion method, and wavelet expansion.

I. INTRODUCTION

In this paper we propose a highly performing parallel numerical method to solve an acoustic time dependent scattering problem involving a realistic smart obstacle. The smart obstacle considered is an obstacle that when hit by an incoming acoustic wave and reacts circulating on its boundary a pressure current (i.e., a field that is dimensionally pressure divided by time) in order to generate a virtual image of a possibly different obstacle (i.e., a ghost obstacle) in a location in space different from its actual one. That is, this kind of smart obstacle when hit by an incoming wave generates a scattered field that, outside a suitable set containing the smart obstacle and the ghost obstacle in the apparent location, resembles to the field scattered in the same circumstances by the ghost obstacle located in the apparent location that is in a position in space different from the position of the obstacle.

Let \mathbf{R} be the set of real numbers and \mathbf{R}^3 be the three dimensional real Euclidean space, the acoustic time dependent direct scattering problem involving the smart obstacle that we want to solve can be stated as follows:

Given an incoming acoustic field propagating in \mathbf{R}^3 , an obstacle $\Omega \subset \mathbf{R}^3$ non empty characterized by an acoustic boundary impedance χ , a ghost obstacle $\Omega_G \subset \mathbf{R}^3$ non empty characterized by an acoustic boundary impedance χ_G such that $\Omega \cap \Omega_G = \emptyset$ and a set $\Omega_\epsilon \subset \mathbf{R}^3$, such that $\Omega, \Omega_G \subset \Omega_\epsilon$, find a pressure current circulating on the boundary of Ω such that the field scattered by Ω when hit by the incoming acoustic field appears, outside Ω_ϵ , "as similar as possible" to the field scattered in the same circumstances by Ω_G .

For simplicity in the numerical examples presented in Section IV we limit our attention to the case when Ω_G is the set Ω translated in space and $\chi = \chi_G$ is a constant. We denote with $\partial\Omega$, $\partial\Omega_G$ the boundary of Ω and Ω_G respectively. This is the formulation of the ghost obstacle scattering problem considered in the numerical examples and it is a simplified version of a more general formulation of the problem that is given in Section II. Indeed, in the numerical examples we solve the ghost obstacle scattering problem in this simplified formulation since we consider problems that are already difficult for other reasons. In fact we consider problems that involve obstacles with complex geometry, that is realistic obstacles, and incoming waves of small wavelengths.

We formulate the ghost obstacle scattering problem as an optimal control problem for the wave equation and, under suitable assumptions, applying the Pontryagin maximum principle, we derive the first order necessary optimality condition relative to the optimal control problem considered. This condition is formulated as an exterior value problem for two coupled wave equations. Assuming that the incoming and the scattered fields and some auxiliary variables can be represented as superposition of time harmonic waves, we reduce the solution of this exterior problem to the solution of a set of exterior problems for two coupled Helmholtz equations. Finally using a perturbation expansion known as operator expansion method (see for example [1, 2]) we reduce the solution of this set of exterior problems for two coupled Helmholtz equations to the solution of a set of systems of first kind integral equations. This approach has been used to solve several direct acoustic and electromagnetic scattering problems involving several kinds of smart obstacles (i.e., undetectable obstacles [2], masked obstacles [3, 4, 5], ghost obstacles [6, 7]). Moreover some attempts to solve inverse acoustic scattering problems involving smart obstacles with ad hoc methods have been made with promising results (i.e.: for furtive and masked obstacles [8, 9] and for ghost obstacles [10, 11]).

A common feature of the work contained in the papers mentioned previously is that the numerical methods proposed assume implicitly that the smart obstacles considered must have simple geometries. In particular they assume that their shape must be not too far from being the shape of a sphere and that the incoming waves used to illuminate the obstacles must be a superposition of time harmonic waves with wavelengths not too small, let us say approximately not smaller than the characteristic length of the obstacles. These assumptions are due to the following facts: the “special” surfaces used in the development of the operator expansion method are chosen to be surfaces of spheres and the set of coupled integral equations coming from the first order optimality condition is solved projecting the systems of integral equations on a vector space generated by a finite subset of the spherical harmonic functions (see [12], p. 77). The use of spherical surfaces as “special” surfaces of the operator expansion

method and of the spherical harmonic functions as function basis to approximate the integral equations makes the corresponding computational method very efficient. In fact this method reduces the solution of the integral equations to the solution of diagonal systems of linear equations. However, it has some disadvantages, one of them is that in practical computations only the first few hundreds spherical harmonic functions can be used so that only linear systems involving few hundreds equations and unknowns can be considered. That is in the scattering problems that can be solved satisfactorily using spherical surfaces as “special” surfaces and the spherical harmonic functions as function basis, the obstacles must have a shape not too far from being the shape of a sphere and the ratios between the characteristic length of the obstacles and the wavelengths present in the Fourier decomposition of the incoming field considered must be at most of a few units.

Moreover, the first order necessary optimality condition given in [6, 7] for the direct ghost scattering problem is derived assuming that Ω and Ω_ϵ are star-like obstacles with respect to the same point and that the set Ω_ϵ is a “magnification” of the obstacle Ω itself. This last assumption in [6, 7] is used to make an expansion involving the surface $\partial\Omega_\epsilon$, boundary of Ω_ϵ , using as “base point” the surface $\partial\Omega$ to get a set of integral equations on $\partial\Omega$. These assumptions restrict the choice of the shape of the smart obstacles and the choice of the distance between the smart and the ghost obstacle that can be considered. In fact, only when the distance between the smart and the ghost obstacle is sufficiently small we have that the expansion involving the surface $\partial\Omega_\epsilon$ mentioned above is convergent.

In this paper we overcome these restrictions giving a new formulation of the first order necessary optimality condition. In particular we remove the assumptions that the set Ω and the set Ω_ϵ are starlike with respect to the same point and that Ω_ϵ is a magnification of Ω . Moreover we remove the assumptions that the “special” surfaces of the operator expansion method are spherical surfaces and that Ω is starlike. As a consequence are removed the restrictions that the smart obstacles considered must have a shape not too far from being the shape of a sphere and that the wavelengths of the time harmonic waves contained in the Fourier decomposition of the incoming field are at least of the same order of magnitude of the characteristic length of the obstacles. A first attempt of removing the restrictions on the shape of the scatterer and on the wavelengths of the time harmonic waves contained in the incoming field in the case of smart obstacles that pursue the goal of being undetectable has been made in [13]. In particular in [13] the set of the coupled integral equations coming from the first order necessary optimality condition of the control problem associated to the furtivity problem is derived and is solved discretizing the integral equations using a wavelet basis introduced in [10]. The use of this wavelet basis makes possible

to solve with affordable computing resources scattering problems involving realistic obstacles when the ratio between the characteristic dimension of the obstacle and the wavelength of the incoming wave goes up to (approximately) sixty at the price of solving non diagonal sparse linear systems having a condition number that increases when the number of unknowns increases. These sparse linear systems contain hundreds of thousands or millions of unknowns and equations. The ghost scattering problem considered in this paper is more difficult than the furtivity problem studied in [13]. In fact it requires a reformulation of the optimal control problem and the use of wavelet bases with improved sparsification properties able to approximate the integral operators involved in the integral equations coming from the first order necessary optimality condition with very sparse matrices. Hence, in this paper, a new wavelet basis, introduced in [14], is used to approximate the set of coupled integral equations coming from the new formulation of the first order optimality condition for the acoustic ghost obstacle scattering problem. This new wavelet basis is made of piecewise constant functions, and generalizes the Haar's basis. Furthermore, the computation of the matrix elements of the matrices that approximate the integral operators consists in the computation of four dimensional integrals independent one from the other. This type of computation is very well suited for parallel computing or even for distributed computing. The computation of these matrix elements is by far the dominant part of the computation in the solution of the ghost obstacle scattering problem when the integral equations that translate the optimal control problem must be approximated in high dimensional vector spaces. Concluding we can say that we have developed an efficient computational method that reduces the solution of the direct ghost obstacle scattering problem involving realistic obstacles and small wavelengths (see Section IV where a simplified version of the NASA space shuttle is considered as obstacle) to the solution of a set of sparse linear systems of equations with hundreds of thousands or millions of unknowns and equations that can be stored and solved using affordable computing resources. The computational method takes care of the ill-conditioning of the sparse linear systems obtained solving them with an iterative procedure that uses suitably chosen starting points. Thank to the use of a parallel implementation of the computational method based on FORTRAN 77 as programming language, on MPI as message passing library, to the use of the SP5 IBM machine with 168 processors (144 processors dedicated to batch running) of CASPUR (Roma, Italy) computing center and to the use of stereographic and virtual reality animations to represent the numerical results obtained, we can solve efficiently very difficult scattering problems and we can represent satisfactorily the results obtained. Some stereographic and virtual reality applications relative to numerical experiments on test problems can be found in the website

<http://www.econ.univpm.it/recchioni/scattering/w16>.

A more general reference to the work in acoustic and electromagnetic scattering of the authors and of their coauthors is the website: <http://www.econ.univpm.it/recchioni/scattering>.

In Section II we formulate the time dependent ghost obstacle scattering problem as an optimal control problem for the wave equation and we derive the corresponding first order optimality condition using the Pontryagin maximum principle (see [7]). In Section III, under suitable assumptions, we reduce the first order optimality condition derived in Section II first to a set of time harmonic problems for a system of two coupled Helmholtz equations and later to a set of systems of integral equations. Moreover we describe the algorithm developed to solve the systems of integral equations using a wavelet basis introduced in [14]. Finally, in Section IV starting from synthetic data the algorithm discussed in Section III is used to solve numerically in some test cases the ghost obstacle scattering problem.

II. THE TIME DEPENDENT GHOST OBSTACLE DIRECT SCATTERING PROBLEM

Let \mathbf{C} be the set of complex numbers, for $\eta \in \mathbf{C}$ let $|\eta|$, $\bar{\eta}$ denote the modulus and the complex conjugate of η respectively. Let $\underline{x} = (x, y, z)^T \in \mathbf{R}^3$ be a generic vector where the superscript T means transposed, (\cdot, \cdot) be the Euclidean scalar product in \mathbf{R}^3 and $\|\cdot\|$ be the corresponding Euclidean vector norm. In the following with abuse of notation occasionally we will use the real Euclidean scalar product of complex vectors.

Let us formulate the scattering problem that we want to study. Let $\Omega \subset \mathbf{R}^3$, $\Omega_G \subset \mathbf{R}^3$ be two bounded simply connected open sets with locally Lipschitz boundaries $\partial\Omega$, $\partial\Omega_G$, and let $\bar{\Omega}$ and $\bar{\Omega}_G$ be their closures. Furthermore, let Ω , Ω_G be such that: $\Omega \neq \emptyset$, $\Omega_G \neq \emptyset$ and $\Omega \cap \Omega_G = \emptyset$. We denote with $\underline{n}(\underline{x}) = (n_1(\underline{x}), n_2(\underline{x}), n_3(\underline{x}))^T \in \mathbf{R}^3$, $\underline{x} \in \partial\Omega$, the outward unit normal vector to $\partial\Omega$ in $\underline{x} \in \partial\Omega$. Since Ω has a locally Lipschitz boundary $\underline{n}(\underline{x})$, $\underline{x} \in \partial\Omega$, exists almost everywhere (see [15] Lemma 2.42 p. 88); similar statements hold for the outward unit normal vector to $\partial\Omega_G$.

We assume that Ω and Ω_G are characterized by constant acoustic boundary impedances $\chi \geq 0$ and $\chi_G \geq 0$ respectively. The case $\chi = +\infty$ and/or $\chi_G = +\infty$ (i.e.: the case of acoustically hard obstacles) can be treated with simple modifications of the formulae that follow. We refer to $(\Omega; \chi)$ as to the obstacle, and to $(\Omega_G; \chi_G)$ as to the ghost obstacle. Without loss of generality, we can assume that the origin of the coordinate system lies in Ω .

We consider an acoustic incident wave $u^i(\underline{x}, t)$, $(\underline{x}, t) \in \mathbf{R}^3 \times \mathbf{R}$, propagating in a homogeneous isotropic medium in equilibrium, with no source terms present, satisfying the wave equation in $\mathbf{R}^3 \times \mathbf{R}$ with wave propagation velocity $c > 0$. We denote with $u^s(\underline{x}, t)$, $(\underline{x}, t) \in (\mathbf{R}^3 \setminus \bar{\Omega}) \times \mathbf{R}$, and with $u_G^s(\underline{x}, t)$, $(\underline{x}, t) \in$

$(\mathbf{R}^3 \setminus \overline{\Omega_G}) \times \mathbf{R}$, the waves scattered, respectively, by the obstacle $(\Omega; \chi)$ and by the ghost obstacle $(\Omega_G; \chi_G)$ when hit by $u^i(\mathbf{x}, t)$, $(\mathbf{x}, t) \in \mathbf{R}^3 \times \mathbf{R}$.

The scattered acoustic field $u^s(\mathbf{x}, t)$, $(\mathbf{x}, t) \in (\mathbf{R}^3 \setminus \overline{\Omega}) \times \mathbf{R}$, when the obstacle Ω is not smart (i.e. is an obstacle that does not react to the incident wave circulating a pressure current on its boundary to pursue a goal) is defined as the solution of the following exterior problem for the wave equation (see [1]),

$$\Delta u^s(\underline{x}, t) - \frac{1}{c^2} \frac{\partial^2 u^s}{\partial t^2}(\underline{x}, t) = 0, \quad (\underline{x}, t) \in (\mathbf{R}^3 \setminus \overline{\Omega}) \times \mathbf{R} \quad (1)$$

with the boundary condition (see [12] p. 66),

$$-\frac{\partial u^s}{\partial t}(\underline{x}, t) + c\chi \frac{\partial u^s}{\partial \underline{n}(\underline{x})} = g(\underline{x}, t), \quad (\underline{x}, t) \in \partial\Omega \times \mathbf{R} \quad (2)$$

where $g(\underline{x}, t)$ is given by,

$$g(\underline{x}, t) = \frac{\partial u^i}{\partial t}(\underline{x}, t) - c\chi \frac{\partial u^i}{\partial \underline{n}(\underline{x})}(\underline{x}, t), \quad (\underline{x}, t) \in \partial\Omega \times \mathbf{R} \quad (3)$$

the condition at infinity,

$$u^s(\underline{x}, t) = O\left(\frac{1}{r}\right), \quad r \rightarrow +\infty, \quad t \in \mathbf{R} \quad (4)$$

and the radiation condition,

$$\frac{\partial u^s}{\partial r}(\underline{x}, t) + \frac{1}{c} \frac{\partial u^s}{\partial t}(\underline{x}, t) = o\left(\frac{1}{r}\right), \quad r \rightarrow +\infty, \quad t \in \mathbf{R} \quad (5)$$

where $r = \|\underline{x}\|$, $\underline{x} \in \mathbf{R}^3$, $\Delta = \frac{\partial^2}{\partial x^2} + \frac{\partial^2}{\partial y^2} + \frac{\partial^2}{\partial z^2}$ is the Laplace operator and $O(\cdot)$ and $o(\cdot)$ are the Landau symbols. We note that $g(\underline{x}, t)$, $(\underline{x}, t) \in \partial\Omega \times \mathbf{R}$, is defined almost everywhere, and that the boundary condition of equation (2) can be adapted to deal with the limit case of acoustically hard obstacles, i.e. obstacles such that $\chi = +\infty$ (see [1, 2]). The obstacle $(\Omega; \chi)$ that scatters the field u^s solution of equations (1), (2), (4), and (5) is called passive obstacle. The field $u_G^s(\mathbf{x}, t)$, $(\mathbf{x}, t) \in (\mathbf{R}^3 \setminus \overline{\Omega_G}) \times \mathbf{R}$, scattered by the (passive) ghost obstacle is defined as the solution of equations (1), (2), (4), and (5) when we replace Ω with Ω_G and χ with χ_G . Note that we always consider the ghost obstacle $(\Omega_G; \chi_G)$ as a passive obstacle.

Remember that in the ghost obstacle problem the smart obstacle $(\Omega; \chi)$ when hit by an incoming wave tries to generate a scattered wave that resembles, outside a given set containing Ω and Ω_G , to the wave scattered by $(\Omega_G; \chi_G)$ in the same circumstances. Our goal is to model the ghost obstacle problem as an optimal control problem for the wave equation introducing a control variable $\psi(\mathbf{x}, t)$, $(\mathbf{x}, t) \in \partial\Omega \times \mathbf{R}$, acting on the boundary of the obstacle. This is done replacing the boundary condition of equation (2) with the following boundary condition,

$$-\frac{\partial u^s}{\partial t}(\underline{x}, t) + c\chi \frac{\partial u^s}{\partial \underline{n}(\underline{x})} = g(\underline{x}, t) + (1 + \chi)\psi(\underline{x}, t), \quad (\underline{x}, t) \in \partial\Omega \times \mathbf{R}. \quad (6)$$

We note that the physical dimension of the control function ψ is pressure divided by time, so that we call ψ ‘‘pressure current’’.

Let Ω_ϵ be a bounded simply connected open set containing Ω and Ω_G with locally Lipschitz boundary $\partial\Omega_\epsilon$ and let $ds_{\partial\Omega_\epsilon}$, $ds_{\partial\Omega}$ be the surface measures on $\partial\Omega_\epsilon$ and $\partial\Omega$ (see [15] Lemma 1.1 p. 119-120), respectively.

As done in [7, 6] we define the cost functional,

$$F_{\lambda, \mu, \epsilon}(\psi) = \int_{\mathbf{R}} dt \left\{ \int_{\partial\Omega_\epsilon} (1 + \chi)\lambda c [u^s(\underline{x}, t) - u_G^s(\underline{x}, t)]^2 ds_{\partial\Omega_\epsilon}(\underline{x}) + \int_{\partial\Omega} (1 + \chi)\mu \varsigma \psi^2(\mathbf{x}, t) ds_{\partial\Omega}(\underline{x}) \right\} \quad (7)$$

where $\lambda \geq 0$, $\mu \geq 0$ are dimensionless constants such that $\lambda + \mu = 1$, and ς is a nonzero positive dimensional constant. Note that in the first addendum of equation (7) we have introduced as a factor the propagation velocity c that does not appear in the functional used in [6, 7], the presence of this factor simplifies some of the formulae that follow. We model the direct ghost obstacle scattering problem via the following optimal control problem,

$$\min_{\psi \in \mathcal{C}} F_{\lambda, \mu, \epsilon}(\psi). \quad (8)$$

Subject to the constraints of equations (1), (4), (5), and (6). The set \mathcal{C} is the space of the admissible controls and is a vector space that we leave unspecified in this paper (see [7] for further details). The obstacle $(\Omega; \chi)$ that generates the scattered field u^s solution of equations (8), (1), (4), (5), and (6) is a smart (or active) obstacle that we call of ghost obstacle type.

As shown in [2, 7] the cases $\mu = 0$ and $\mu = 1$ are trivial. The choice of the cost functional of equation (7) is motivated by the fact that when $0 < \mu < 1$ we have $\lambda > 0$, that is, when $0 < \mu < 1$ the minimization of $F_{\lambda, \mu, \epsilon}$ makes small on $\partial\Omega_\epsilon$ for all times the difference between the field scattered by the smart obstacle and the field scattered by the ghost obstacle and makes small on $\partial\Omega$ for all times the control function used to achieve this goal. Note that forcing the two scattered fields to be similar on $\partial\Omega_\epsilon$ for all times implies that they remain similar in $\mathbf{R}^3 \setminus \overline{\Omega_\epsilon}$ for all times. So that an observer located in $\mathbf{R}^3 \setminus \overline{\Omega_\epsilon}$ that observes the scattered field is induced to believe that the obstacle generating the scattered field is the ghost obstacle $(\Omega_G; \chi_G)$ instead than the obstacle $(\Omega; \chi)$. From now on we restrict our attention to the case $0 < \mu < 1$.

We note that the functional of equation (7) is defined via two integrals, one integral on the boundary of Ω and

the other integral on the boundary of Ω_ϵ . This fact makes difficult to write conveniently the first order optimality condition associated to the optimal control problem of equations (8), (1), (4), (5), and (6). In reference [7] this difficulty has been solved assuming that the boundary of Ω is a star like surface and that the boundary of Ω_ϵ is obtained by a simple transformation of the boundary of Ω that previously we have called magnification. In this paper we modify this assumption since we deal with obstacles (see Fig. 3(b)) whose boundaries are not starlike surfaces with respect to a point in their interior.

The numerical experiments presented in this paper are done using cylindrical coordinates since the simplified NASA space shuttle (Fig. 3(b)), that is the obstacle considered in Section IV, can be described conveniently using these coordinates. So that, for simplicity, we use cylindrical coordinates also in this section and in Section III in the exposition of the solution method. When necessary more general curvilinear coordinate systems can be considered as shown, for example, in [16].

Let us introduce the canonical cylindrical coordinate system in \mathbf{R}^3 , that is (r_1, ϕ, z) , with origin in a point in the interior of the smart obstacle that will be specified later and let $\hat{\phi} = (\cos \phi, \sin \phi, 0)^T \in \mathbf{R}^3$, $\phi \in [0, 2\pi)$ and $\hat{z} = (0, 0, z)^T = z\mathbf{e}_3 \in \mathbf{R}^3$, $z \in \mathbf{R}$, $\mathbf{e}_3 = (0, 0, 1)^T \in \mathbf{R}^3$. Note that with abuse of notation, in order to keep the exposition simple in formulae equations (9)-(34) we have used the coordinates (r_1, ϕ, z) to denote several cylindrical coordinate systems obtained one from the others with suitable translations, in the specific contexts considered the coordinate systems used will be understandable. We assume that:

(a) The obstacle $(\Omega; \chi)$ is given by,

$$\begin{aligned} \Omega &= \{ \underline{x} = (r_1 \cos \phi, r_1 \sin \phi, z)^T \quad (9) \\ &= r_1 \hat{\phi} + z\mathbf{e}_3 \in \mathbf{R}^3 \mid 0 \leq r_1 < \xi(\phi, z), \\ &\phi \in [0, 2\pi), z \in [z_i, z_f] \}, \quad (10) \end{aligned}$$

where z_i, z_f are two real numbers such that $z_i < z_f$ and $\xi(\phi, z) > 0$, $\phi \in [0, 2\pi)$, $z \in (z_i, z_f)$ is a single valued function defined in $[0, 2\pi) \times [z_i, z_f]$ sufficiently regular to make sense out for the manipulations that follow. As a consequence of equation (9) we have,

$$\begin{aligned} \partial\Omega &= \{ \underline{x} = (r_1 \cos \phi, r_1 \sin \phi, z)^T = \\ &\xi(\phi, z) \hat{\phi} + z\mathbf{e}_3 \in \mathbf{R}^3, \phi \in [0, 2\pi), z \in [z_i, z_f] \}. \quad (11) \end{aligned}$$

(b) The sets Ω_G and $\partial\Omega_G$ are given by,

$$\begin{aligned} \Omega_G &= \{ \underline{x} = \underline{p}_G + (r_1 \cos \phi, r_1 \sin \phi, s_G(z))^T = \\ &\underline{p}_G + r_1 \hat{\phi} + s_G(z)\mathbf{e}_3 \in \mathbf{R}^3 \mid 0 \leq r_1 < \xi_G(\phi, s_G(z)), \\ &\phi \in [0, 2\pi), z \in [z_i, z_f] \}, \quad (12) \end{aligned}$$

and

$$\begin{aligned} \partial\Omega_G &= \{ \underline{x} = \underline{p}_G + (r_1 \cos \phi, r_1 \sin \phi, s_G(z))^T = \\ &\underline{p}_G + \xi_G(\phi, s_G(z)) \hat{\phi} + s_G(z)\mathbf{e}_3 \in \mathbf{R}^3, \\ &\phi \in [0, 2\pi), z \in [z_i, z_f] \}, \quad (13) \end{aligned}$$

where $s_G(z) = z_i^G + (z - z_i)(z_f^G - z_i^G)/(z_f - z_i)$ is a linear function of z , z_i^G, z_f^G are constants such that $z_i^G < z_f^G$, $\xi_G(\phi, s_G(z))$, $\phi \in [0, 2\pi)$, $z \in [z_i, z_f]$ is a single valued function and $\underline{p}_G \in \mathbf{R}^3$ is a suitable vector (see Fig. 1).

(c) The sets Ω_ϵ and $\partial\Omega_\epsilon$ are given by,

$$\begin{aligned} \Omega_\epsilon &= \{ \underline{x} = \underline{p} + (r_1 \cos \phi, r_1 \sin \phi, s(z))^T = \\ &\underline{p} + r_1 \hat{\phi} + s(z)\mathbf{e}_3 \in \mathbf{R}^3, 0 \leq r_1 < \xi_\epsilon(\phi, s(z)), \\ &\phi \in [0, 2\pi), z \in [z_i, z_f] \}, \quad (14) \end{aligned}$$

and

$$\begin{aligned} \partial\Omega_\epsilon &= \{ \underline{x} = \underline{p} + (r_1 \cos \phi, r_1 \sin \phi, s(z))^T = \\ &\underline{p} + \xi_\epsilon(\phi, s(z)) \hat{\phi} + s(z)\mathbf{e}_3 \in \mathbf{R}^3, \\ &\phi \in [0, 2\pi), z \in [z_i, z_f] \}, \quad (15) \end{aligned}$$

where $s(z) = z_i^* + (z - z_i)(z_f^* - z_i^*)/(z_f - z_i)$ is a linear function of z and z_i^*, z_f^* are constants such that $z_i^* < z_f^*$. Finally, $\underline{p} \in \mathbf{R}^3$ is a suitable vector (see Fig. 1) and ξ_ϵ is a single valued function such that $\Omega \subset \Omega_\epsilon$ and $\Omega_G \subset \Omega_\epsilon$.

Figure 1 shows an example of the ghost obstacle experiment in a simple situation where Ω is a sphere of center the origin and Ω_G is a translation of Ω . Note that only for simplicity we have chosen the origin of the cylindrical coordinate system in the center of mass of the smart obstacle.

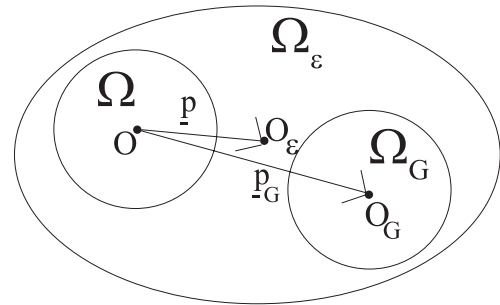


Fig. 1. The ghost obstacle experiment: Ω obstacle, Ω_G ghost obstacle, Ω_ϵ auxiliary set, O point contained in Ω and origin of the coordinate system, O_G point contained in Ω_G , O_ϵ point contained in Ω_ϵ .

Note that in a suitable cylindrical coordinate system with origin in the point O_G of the set Ω_G or in the point O_ϵ of the set Ω_ϵ we have respectively the following representation formulae for Ω_G and Ω_ϵ ,

$$\begin{aligned} \Omega_G &= \{ \underline{x} = (r_1 \cos \phi, r_1 \sin \phi, z)^T = \\ &r_1 \hat{\phi} + z\mathbf{e}_3 \in \mathbf{R}^3 \mid 0 \leq r_1 < \xi_G(\phi, z), \\ &\phi \in [0, 2\pi), z \in [z_i^G, z_f^G] \}, \quad (16) \end{aligned}$$

and

$$\begin{aligned} \Omega_\epsilon &= \{ \underline{x} = (r_1 \cos \phi, r_1 \sin \phi, z)^T = \\ & r_1 \hat{\phi} + z \underline{e}_3 \in \mathbf{R}^3 \mid 0 \leq r_1 < \xi_\epsilon(\phi, z), \\ & \phi \in [0, 2\pi), z \in [z_i^*, z_f^*] \}. \end{aligned} \quad (17)$$

Remember that as already said with abuse of notation in the previous formulae, (r_1, ϕ, z) denotes several cylindrical coordinate systems and that given Ω , Ω_G such that $\Omega \neq \emptyset$, $\Omega_G \neq \emptyset$ and $\Omega \cap \Omega_G = \emptyset$, we must choose Ω_ϵ such that $\Omega \subset \Omega_\epsilon$ and $\Omega_G \subset \Omega_\epsilon$.

Under assumptions (a) and (b) and other technical assumptions (see [2, 7]) applying the Pontryagin maximum principle, we find that the optimal scattered field $\tilde{u}^s(\underline{x}, t)$, $(\underline{x}, t) \in (\mathbf{R}^3 \setminus \bar{\Omega}) \times \mathbf{R}$, and the corresponding adjoint variable $\tilde{\varphi}(\underline{x}, t)$, $(\underline{x}, t) \in (\mathbf{R}^3 \setminus \bar{\Omega}) \times \mathbf{R}$, satisfy the first-order necessary optimality condition associated to the optimal control problem of equations (8), (1), (4), (5), and (6). That is, they are the solution of the following exterior problem for a system of two coupled wave equations,

$$\Delta \tilde{u}^s(\underline{x}, t) - \frac{1}{c^2} \frac{\partial^2 \tilde{u}^s}{\partial t^2}(\underline{x}, t) = 0, \quad (\underline{x}, t) \in (\mathbf{R}^3 \setminus \bar{\Omega}) \times \mathbf{R} \quad (18)$$

$$\tilde{u}^s(\underline{x}, t) = O\left(\frac{1}{r}\right), \quad r \rightarrow +\infty, \quad t \in \mathbf{R}, \quad (19)$$

$$\frac{\partial \tilde{u}^s}{\partial r}(\underline{x}, t) + \frac{1}{c} \frac{\partial \tilde{u}^s}{\partial t}(\underline{x}, t) = o\left(\frac{1}{r}\right), \quad r \rightarrow +\infty, \quad t \in \mathbf{R}, \quad (20)$$

$$\begin{aligned} -\frac{\partial \tilde{u}^s}{\partial t}(\underline{x}, t) + c\chi \frac{\partial \tilde{u}^s}{\partial \underline{n}(\underline{x})}(\underline{x}) &= g(\underline{x}, t) - \frac{(1+\chi)}{\varsigma} \tilde{\varphi}(\underline{x}, t), \\ (\underline{x}, t) \in \partial\Omega \times \mathbf{R}, \end{aligned} \quad (21)$$

$$\Delta \tilde{\varphi}(\underline{x}, t) - \frac{1}{c^2} \frac{\partial^2 \tilde{\varphi}}{\partial t^2}(\underline{x}, t) = 0, \quad (\underline{x}, t) \in (\mathbf{R}^3 \setminus \bar{\Omega}) \times \mathbf{R}, \quad (22)$$

$$\tilde{\varphi}(\underline{x}, t) = O\left(\frac{1}{r}\right), \quad r \rightarrow +\infty, \quad t \in \mathbf{R}, \quad (23)$$

$$\frac{\partial \tilde{\varphi}}{\partial r}(\underline{x}, t) - \frac{1}{c} \frac{\partial \tilde{\varphi}}{\partial t}(\underline{x}, t) = o\left(\frac{1}{r}\right), \quad r \rightarrow +\infty, \quad t \in \mathbf{R}, \quad (24)$$

$$\begin{aligned} -\mu \frac{\partial \tilde{\varphi}}{\partial t}(\underline{x}, t) - c\chi\mu \frac{\partial \tilde{\varphi}}{\partial \underline{n}(\underline{x})}(\underline{x}) &= \\ -\lambda c(1+\chi) f_\epsilon(\underline{x})(\tilde{u}^s(\underline{p}_\epsilon(\underline{x}), t) - u_G^s(\underline{p}_\epsilon(\underline{x}), t)), \\ (\underline{x}, t) \in \partial\Omega \times \mathbf{R}, \end{aligned} \quad (25)$$

$$\lim_{t \rightarrow -\infty} \tilde{u}^s(\underline{x}, t) = 0, \quad \underline{x} \in \mathbf{R}^3 \setminus \bar{\Omega}, \quad (26)$$

$$\lim_{t \rightarrow +\infty} \tilde{\varphi}(\underline{x}, t) = 0, \quad \underline{x} \in \mathbf{R}^3 \setminus \Omega, \quad (27)$$

where $\underline{p}_\epsilon(\underline{x})$ is a point belonging to $\partial\Omega_\epsilon$ given by,

$$\begin{aligned} \underline{p}_\epsilon(\underline{x}) &= \frac{\xi_\epsilon(\phi, s(z))}{\xi(\phi, z)} [\underline{x} - (\underline{x}, \underline{e}_3)\underline{e}_3] + s((\underline{x}, \underline{e}_3))\underline{e}_3, \\ \underline{x} &= \xi \hat{\phi} + z \underline{e}_3 \in \partial\Omega \end{aligned} \quad (28)$$

where $s(z) = z_i^* + (z - z_i)(z_f^* - z_i^*) / (z_f - z_i)$, $z \in [z_i, z_f]$, and $f_\epsilon(\underline{x})$, $\underline{x} \in \partial\Omega$, is the function defined by,

$$\begin{aligned} f_\epsilon(\underline{x}(\phi, z)) &= \frac{v_\epsilon(\phi, z)}{v(\phi, z)}, \quad \underline{x} = \xi(\phi, z)\hat{\phi} + z\underline{e}_3 \in \partial\Omega, \\ \phi &\in [0, 2\pi), \quad z \in [z_i, z_f] \end{aligned} \quad (29)$$

with

$$\begin{aligned} v(\theta, \phi) &= \\ \left[\xi^2(\phi, z) + \left(\frac{\partial \xi}{\partial \phi} \right)^2(\phi, z) + \xi^2(\phi, z) \left(\frac{\partial \xi}{\partial z} \right)^2(\phi, z) \right]^{\frac{1}{2}}, \\ \phi &\in [0, 2\pi), \quad z \in [z_i, z_f], \end{aligned} \quad (30)$$

$$\begin{aligned} v_\epsilon(\theta, \phi) &= \frac{(z_f^* - z_i^*)}{(z_f - z_i)} \cdot \left[\xi_\epsilon^2(\phi, s(z)) + \right. \\ \left. \left(\frac{\partial \xi_\epsilon}{\partial \phi} \right)^2(\phi, s(z)) + \xi_\epsilon^2(\phi, s(z)) \left(\frac{\partial \xi_\epsilon}{\partial s(z)} \right)^2(\phi, s(z)) \right]^{\frac{1}{2}}, \\ \phi &\in [0, 2\pi), \quad z \in [z_i, z_f]. \end{aligned} \quad (31)$$

The relation between $\tilde{\varphi}$ solution of equations (18)-(27) and the optimal control $\tilde{\psi}$ solution of problem of equations (8), (1), (4), (5), and (6) is the following one,

$$\tilde{\psi}(\underline{x}, t) = -\frac{1}{\varsigma} \tilde{\varphi}(\underline{x}, t), \quad (\underline{x}, t) \in \partial\Omega \times \mathbf{R}. \quad (32)$$

For future convenience, we point out that,

$$ds_{\partial\Omega} = v(\phi, z) d\phi dz, \quad \phi \in [0, 2\pi), \quad z \in [z_i, z_f] \quad (33)$$

and

$$ds_{\partial\Omega_\epsilon} = v_\epsilon(\phi, z) d\phi dz, \quad \phi \in [0, 2\pi), \quad z \in [z_i, z_f]. \quad (34)$$

Note that in order to guarantee conditions of equations (26) and (27) we must choose the incoming field in a suitable class of functions (see [2]). This will be done in Section III. We note that the boundary conditions of equations (21) and (25) can be slightly modified to deal with the limit case $\chi = +\infty$.

III. THE NUMERICAL SOLUTION OF THE FIRST ORDER OPTIMALITY CONDITION

Let $B = \{ \underline{x} \in \mathbf{R}^3 \mid \|\underline{x}\| < 1 \}$ and ∂B be the boundary of B . We assume that u^i , \tilde{u}^s , u_G^s and $\tilde{\varphi}$ can be approximated in a compact subset of the time axis by finite sums of time harmonic waves, that is,

$$\begin{aligned} u^i(\underline{x}, t) &\approx \sum_{i=1}^{N_1} \sum_{j=1}^{N_2} \left[a_{i,j} e^{-i\omega_i t} e^{i\omega_i(\underline{x}, \underline{\alpha}_j)/c} \right] \\ (\underline{x}, t) &\in \mathbf{R}^3 \times \mathbf{R}, \end{aligned} \quad (35)$$

$$\begin{aligned} \tilde{u}^s(\mathbf{x}, t) &\approx \sum_{i=1}^{N_1} \sum_{j=1}^{N_2} \left[a_{i,j} e^{-\imath \omega_i t} u_{\omega_i, \underline{\alpha}_j}^s(\mathbf{x}) \right], \\ (\mathbf{x}, t) &\in (\mathbf{R}^3 \setminus \bar{\Omega}) \times \mathbf{R}, \end{aligned} \quad (36)$$

$$\begin{aligned} u_G^s(\mathbf{x}, t) &\approx \sum_{i=1}^{N_1} \sum_{j=1}^{N_2} \left[a_{i,j} e^{-\imath \omega_i t} u_{G, \omega_i, \underline{\alpha}_j}^s(\mathbf{x}) \right], \\ (\mathbf{x}, t) &\in (\mathbf{R}^3 \setminus \bar{\Omega}) \times \mathbf{R}, \end{aligned} \quad (37)$$

$$\begin{aligned} \tilde{\varphi}(\mathbf{x}, t) &\approx \sum_{i=1}^{N_1} \sum_{j=1}^{N_2} \left[a_{i,j} e^{-\imath \omega_i t} \varphi_{\omega_i, \underline{\alpha}_j}(\mathbf{x}) \right], \\ (\mathbf{x}, t) &\in (\mathbf{R}^3 \setminus \bar{\Omega}) \times \mathbf{R}, \end{aligned} \quad (38)$$

where $\imath \in \mathbf{C}$ is the imaginary unit, N_1, N_2 are positive integers, $a_{i,j} \in \mathbf{R}$, $\omega_i \in \mathbf{R}$, $\underline{\alpha}_j \in \partial B$, $i = 1, 2, \dots, N_1$, $j = 1, 2, \dots, N_2$ are suitable quantities, $u_{G, \omega_i, \underline{\alpha}_j}^s$, $i = 1, 2, \dots, N_1$, $j = 1, 2, \dots, N_2$ are suitable functions and $u_{\omega_i, \underline{\alpha}_j}^s(\mathbf{x})$, $\varphi_{\omega_i, \underline{\alpha}_j}(\mathbf{x})$, $\mathbf{x} \in \mathbf{R}^3 \setminus \Omega$, $i = 1, 2, \dots, N_1$, $j = 1, 2, \dots, N_2$, are functions to be determined. Substituting the right hand side of equations(35)-(38) into equations (18)-(27) and defining $\tilde{\zeta} = c\zeta$ we obtain that the space dependent part $u_{\omega, \underline{\alpha}}^s(\mathbf{x})$, $\mathbf{x} \in \mathbf{R}^3 \setminus \Omega$, of the time harmonic components of \tilde{u}^s , and the space dependent part $\varphi_{\omega, \underline{\alpha}}(\mathbf{x})$, $\mathbf{x} \in \mathbf{R}^3 \setminus \Omega$, of the time harmonic components of $\tilde{\varphi}$, $(\omega, \underline{\alpha}) = (\omega_i, \underline{\alpha}_j)$, $i = 1, 2, \dots, N_1$, $j = 1, 2, \dots, N_2$, are solutions of the following set of systems of Helmholtz: for $i = 1, 2, \dots, N_1$, $j = 1, 2, \dots, N_2$, and $(\omega, \underline{\alpha}) = (\omega_i, \underline{\alpha}_j)$, we have,

$$\left(\Delta u_{\omega, \underline{\alpha}}^s + \frac{\omega^2}{c^2} u_{\omega, \underline{\alpha}}^s \right)(\underline{x}) = 0 \quad (39)$$

$$\left(\Delta \varphi_{\omega, \underline{\alpha}} + \frac{\omega^2}{c^2} \varphi_{\omega, \underline{\alpha}} \right)(\underline{x}) = 0, \underline{x} \in \mathbf{R}^3 \setminus \bar{\Omega}, \quad (40)$$

$$\begin{aligned} \imath \omega u_{\omega, \underline{\alpha}}^s(\underline{x}) + c\chi \frac{\partial u_{\omega, \underline{\alpha}}^s}{\partial \underline{n}(\underline{x})}(\underline{x}) + c \frac{(1+\chi)}{\tilde{\zeta}} \varphi_{\omega, \underline{\alpha}}(\mathbf{x}) &= \\ b_{\omega, \underline{\alpha}}(\underline{x}), \underline{x} \in \partial\Omega, \end{aligned} \quad (41)$$

$$\begin{aligned} \imath \omega \mu \varphi_{\omega, \underline{\alpha}}(\underline{x}) - c\mu\chi \frac{\partial \varphi_{\omega, \underline{\alpha}}}{\partial \underline{n}(\underline{x})}(\underline{x}) + c\lambda(1+\chi) \cdot \\ \left(u_{\omega, \underline{\alpha}}^s(\underline{p}_\epsilon(\underline{x})) - u_{G, \omega, \underline{\alpha}}^s(\underline{p}_\epsilon(\underline{x})) \right) = 0, \underline{x} \in \partial\Omega, \end{aligned} \quad (42)$$

with the conditions at infinity,

$$\frac{\partial u_{\omega, \underline{\alpha}}^s(\underline{x})}{\partial r} - \imath \frac{\omega}{c} u_{\omega, \underline{\alpha}}^s(\underline{x}) = o\left(\frac{1}{r}\right), \quad r \rightarrow +\infty, \quad (43)$$

$$\frac{\partial \varphi_{\omega, \underline{\alpha}}(\underline{x})}{\partial r} + \imath \frac{\omega}{c} \varphi_{\omega, \underline{\alpha}}(\underline{x}) = o\left(\frac{1}{r}\right), \quad r \rightarrow +\infty, \quad (44)$$

where $b_{\omega, \underline{\alpha}}(\mathbf{x}) = -\imath \omega e^{\imath \omega(\mathbf{x}, \underline{\alpha})/c} (1 + \chi(\underline{n}(\mathbf{x}), \underline{\alpha}))$, $\mathbf{x} \in \partial\Omega$. We remind that \underline{p} has been defined in (28).

Using equations (32) and (38) the relation of the adjoint variables $\varphi_{\omega_i, \underline{\alpha}_j}$, $i = 1, 2, \dots, N_1$, $j = 1, 2, \dots, N_2$, with the optimal control variable $\tilde{\psi}$ can be expressed as follows,

$$\begin{aligned} \tilde{\psi}(\mathbf{x}, t) &\approx -\frac{c}{\tilde{\zeta}} \sum_{i=1}^{N_1} \sum_{j=1}^{N_2} a_{i,j} e^{-\imath \omega_i t} \varphi_{\omega_i, \underline{\alpha}_j}(\mathbf{x}), \\ (\mathbf{x}, t) &\in \partial\Omega \times \mathbf{R}, 0 < \mu < 1. \end{aligned} \quad (45)$$

We propose a variation of the operator expansion method

presented in [17] to solve, using affordable computing resources, equations (39)-(44) when $(\Omega; \chi)$ has a complex geometry and at least some of the wavelengths contained in the incoming wave packet of equation (35) (i.e., some of the quantities $|2\pi/(\omega_i/c)|$, $i = 1, 2, \dots, N_1$) are small compared with the characteristic dimension of the obstacle. In the numerical experiments presented in Section IV we consider problems where the ratio between the characteristic dimension of the obstacle and the wavelength of the time harmonic component of the incident waves goes up to approximately sixty.

As done in equation (35) let us consider acoustic incoming time harmonic plane waves whose space dependent part is given by,

$$u_{\omega, \underline{\alpha}}^i(\mathbf{x}) = e^{\imath \omega(\mathbf{x}, \underline{\alpha})/c}, \quad \mathbf{x} \in \mathbf{R}^3 \quad (46)$$

where $c > 0$ is the wave propagation velocity, $\omega \neq 0$ is the frequency of the wave, $\underline{\alpha} \in \partial B$ is the wave propagation direction. Let us define the wave number k as $k = \omega/c$, we remind that $2\pi/|k|$ is the wavelength of the plane wave of equation (46). Later we will choose $\omega = \omega_i$, $i = 1, 2, \dots, N_1$, and $\underline{\alpha} = \underline{\alpha}_j$, $j = 1, 2, \dots, N_2$.

Let us describe briefly the basic steps of the operator expansion method (see [2, 16, 17] for more details). Let (r_1, ϕ, z) be the canonical cylindrical coordinate system introduced in Section II and let us assume that $\partial\Omega$ is given by formula (11). The use of the operator expansion method to solve equations (39)-(44) is based on the following assumptions:

(a₁) there exists a bounded simply connected open set Ω_c such that $\bar{\Omega}_c \subset \Omega$ with locally Lipschitz boundary $\partial\Omega_c$, given by,

$$\begin{aligned} \partial\Omega_c &= \{ \underline{x} = (r_1 \cos \phi, r_1 \sin \phi, z)^T \in \mathbf{R}^3 \mid \\ r_1 &= \xi_c(\phi, z), \phi \in [0, 2\pi), z \in [\tilde{z}_i, \tilde{z}_f] \} \end{aligned} \quad (47)$$

where \tilde{z}_i, \tilde{z}_f are two given real numbers such that $\tilde{z}_i < \tilde{z}_f$, $[\tilde{z}_i, \tilde{z}_f] \subset (z_i, z_f)$ and ξ_c is a single valued function sufficiently regular to make sense out of the formulae that follow. Note that we have: $0 < \xi_c(\phi, z) < \xi(\phi, z)$, $\phi \in [0, 2\pi)$, $z \in (\tilde{z}_i, \tilde{z}_f)$,

(b₁) for $(\omega, \underline{\alpha}) = (\omega_i, \underline{\alpha}_j)$, $i = 1, 2, \dots, N_1$, $j = 1, 2, \dots, N_2$, the functions $u_{\omega, \underline{\alpha}}^s$, $\varphi_{\omega, \underline{\alpha}}$ that solve the exterior problem (39)-(44) can be written as

single layer potentials with density functions (to be determined) supported on $\partial\Omega_c$, that is,

$$u_{\omega,\underline{\alpha}}^s(\mathbf{x}) = \int_{\partial\Omega_c} ds_{\partial\Omega_c}(\mathbf{y}) \Phi_{\underline{\omega}}^s(\mathbf{x}, \mathbf{y}) c_{\omega,\underline{\alpha}}(\mathbf{y}), \quad \mathbf{x} \in \mathbf{R}^3 \setminus \Omega \quad (48)$$

$$\varphi_{\omega,\underline{\alpha}}(\mathbf{x}) = \int_{\partial\Omega_c} ds_{\partial\Omega_c}(\mathbf{y}) \overline{\Phi_{\underline{\omega}}^s(\mathbf{x}, \mathbf{y})} f_{\omega,\underline{\alpha}}(\mathbf{y}), \quad \mathbf{x} \in \mathbf{R}^3 \setminus \Omega, \quad (49)$$

where $ds_{\partial\Omega_c}$ is the surface measure defined on $\partial\Omega_c$ that we assume to be given by: $ds_{\partial\Omega_c}(\mathbf{y}(\phi, z)) = g_c(\phi, z) d\phi dz$, $(\phi, z) \in U' = (0, 2\pi) \times (\tilde{z}_i, \tilde{z}_f)$, where g_c is a sufficiently regular positive function, $\Phi_{\underline{\omega}}^s(\mathbf{x}, \mathbf{y}) = \frac{e^{i\frac{\omega}{c}\|\underline{x}-\underline{y}\|}}{4\pi\|\underline{x}-\underline{y}\|}$, $\underline{x}, \underline{y} \in \mathbf{R}^3$, $\underline{x} \neq \underline{y}$, is the fundamental solution of the Helmholtz operator on \mathbf{R}^3 satisfying the radiation condition (43) and finally $c_{\omega,\underline{\alpha}}(\mathbf{y})$, $f_{\omega,\underline{\alpha}}(\mathbf{y})$, $\mathbf{y} \in \partial\Omega_c$ are the density functions to be determined mentioned previously. We note that $\overline{\Phi_{\underline{\omega}}^s}$, the complex conjugate of $\Phi_{\underline{\omega}}^s$, satisfies the radiation condition (44);

- (c₁) there exists a surface $\partial\Omega_r$ boundary of a bounded simply connected open set Ω_r representable with a formula analogous to formula (11) when we replace the function ξ with a suitable single valued function ξ_r such that $\Omega_c \subset \Omega_r$ and such that the statements contained in (d₁) hold. We refer to the surface $\partial\Omega_r$ as “reference surface”;
- (d₁) let $\mathbf{y}_{\xi_c}(\underline{v}') = (\xi_c(\underline{v}') \cos(\phi'), \xi_c(\underline{v}') \sin(\phi'), z'^T$, $\underline{v}' = (\phi', z')^T \in U'$ denote a (generic) point of $\partial\Omega_c$, we assume that the following perturbative expansions of $u_{\omega,\underline{\alpha}}^s$ and $\varphi_{\omega,\underline{\alpha}}$ hold,

$$u_{\omega,\underline{\alpha}}^s(\mathbf{x}) = \int_{U'} d\underline{v}' g_c(\underline{v}') \left(\Phi_{\underline{\omega}}^s(\mathbf{x}, \mathbf{y}_{\xi_c}(\underline{v}')) \cdot \sum_{s=0}^{+\infty} \tilde{c}_{k,\underline{\alpha},s}(\underline{v}') (\xi(\underline{v}') - \xi_r(\underline{v}'))^s \right), \quad \mathbf{x} \in \mathbf{R}^3 \setminus \Omega \quad (50)$$

$$\varphi_{\omega,\underline{\alpha}}(\mathbf{x}) = \int_{U'} d\underline{v}' g_c(\underline{v}') \left(\overline{\Phi_{\underline{\omega}}^s(\mathbf{x}, \mathbf{y}_{\xi_c}(\underline{v}'))} \cdot \sum_{s=0}^{+\infty} \tilde{f}_{k,\underline{\alpha},s}(\underline{v}') (\xi(\underline{v}') - \xi_r(\underline{v}'))^s \right), \quad \mathbf{x} \in \mathbf{R}^3 \setminus \Omega, \quad (51)$$

where $d\underline{v}' = d\phi' dz'$ is the usual Lebesgue measure on U' . With abuse of notation we require that $\tilde{c}_{k,\underline{\alpha},s}(\xi - \xi_r)^s = O((\xi - \xi_r)^s)$, $\tilde{f}_{k,\underline{\alpha},s}(\xi - \xi_r)^s = O((\xi - \xi_r)^s)$ as $\xi \rightarrow \xi_r$, $s = 0, 1, 2, \dots$

Note that the surfaces $\partial\Omega_c$ and $\partial\Omega_r$ introduced here have been called “special” surfaces of the operator expansion method in Section I. We note that $u_{\omega,\underline{\alpha}}^s$, $\varphi_{\omega,\underline{\alpha}}$ given by equations (48) and (49) satisfy the

Helmholtz equations (39) and (40) and the “radiation” conditions at infinity of equations (43) and (44) for any choice of the density functions $c_{\omega,\underline{\alpha}}$ and $f_{\omega,\underline{\alpha}}$ that make possible differentiation under the integral sign. Using assumptions (a₁)-(d₁), substituting equations (50) and (51) into the boundary conditions (41), (42) and imposing the boundary conditions (41), (42) order by order in perturbation theory we obtain a sequence of systems of integral equations, that is a system made of two integral equations at each order in the expansion in powers of $(\xi - \xi_r)$. In fact remind that $k = \omega/c$ is the wave number of the incoming plane wave and let $U = (0, 2\pi) \times (z_i, z_f)$, $\mathbf{x}_{\xi_r}(\underline{v})$, $\underline{v} \in U$, be a (generic) point belonging to $\partial\Omega_r$, $\nabla_{\mathbf{x}}$ be the gradient operator with respect to $\mathbf{x} \in \mathbf{R}^3$, for $\nu = 0, 1, \dots$ let $\hat{\phi}_k(\underline{v}) = (1/\nu k) \chi n(\underline{x}_{\xi}(\underline{v}))$, $\underline{v} \in U$, $Q_{\nu}(\underline{v}, \mathbf{y}) = \frac{\partial^{\nu}}{\partial r_1^{\nu}} \nabla_{\mathbf{x}} \Phi_k((r_1 \cos \phi, r_1 \sin \phi, z)^T, \mathbf{y}) \big|_{r_1=\xi_r(\underline{v})}$, and $\mathcal{L}^{\nu}(\underline{v}, \mathbf{y}) = \frac{\partial^{\nu}}{\partial r_1^{\nu}} \Phi_k((r_1 \cos \phi, r_1 \sin \phi, z)^T, \mathbf{y}) \big|_{r_1=\xi_r(\underline{v})}$, $\underline{v} \in U$, $\mathbf{y} \in \mathbf{R}^3$, $\mathbf{y} \notin \partial\Omega_r$, arguing as in [16] it can be shown that the solution of problem (39)-(44) can be reduced to the solution of the following set of systems of integral equations in the unknowns $c_{k,\underline{\alpha},s}(\underline{v}') = g_c(\underline{v}') \tilde{c}_{k,\underline{\alpha},s}(\underline{v}') (\xi(\underline{v}') - \xi_r(\underline{v}'))^s$, $\underline{v}' \in U'$, $f_{k,\underline{\alpha},s}(\underline{v}') = g_c(\underline{v}') \tilde{f}_{k,\underline{\alpha},s}(\underline{v}') (\xi(\underline{v}') - \xi_r(\underline{v}'))^s$, $\underline{v}' \in U'$, $s = 0, 1, 2, \dots$,

$$\int_{U'} d\underline{v}' K_{\xi_r, \xi_c}(\underline{v}, \underline{v}') c_{k,\underline{\alpha},s}(\underline{v}') + \frac{(1+\chi)}{\zeta k} \int_{U'} d\underline{v}' \nu \overline{\Phi_k(\underline{x}_{\xi_r}(\underline{v}), \underline{y}_{\xi_c}(\underline{v}'))} f_{k,\underline{\alpha},s}(\underline{v}') = d_{1,k,\underline{\alpha},s}(\underline{v}), \quad \underline{v} = (v_1, v_2)^T \in U, \quad s = 0, 1, 2, \dots \quad (52)$$

$$-\frac{\lambda(1+\chi)}{k} \hat{f}_{\epsilon}(\underline{v}) \int_{U'} d\underline{v}' [\nu c_{k,\underline{\alpha},s}(\underline{v}') \cdot \Phi_k(\underline{p} + \xi_{\epsilon}(v_1, s(v_2)) \hat{\phi}(v_1) + \hat{z}(v_2), \underline{y}_{\xi_c}(\underline{v}'))] + \mu \int_{U'} d\underline{v}' \overline{K_{\xi_r, \xi_c}(\underline{v}, \underline{v}')} f_{k,\underline{\alpha},s}(\underline{v}') = d_{2,k,\underline{\alpha},s}(\underline{v}), \quad \underline{v} = (v_1, v_2)^T \in U, \quad s = 0, 1, 2, \dots, \quad (53)$$

where K_{ξ_r, ξ_c} is given by,

$$K_{\xi_r, \xi_c}(\underline{v}, \underline{v}') = \left[\Phi_k(\underline{x}_{\xi_r}(\underline{v}), \underline{y}_{\xi_c}(\underline{v}')) + \left(\hat{\phi}_k(\underline{v}), (\nabla_{\mathbf{x}} \Phi_k)(\underline{x}_{\xi_r}(\underline{v}), \underline{y}_{\xi_c}(\underline{v}')) \right) \right], \quad \underline{v} \in U, \underline{v}' \in U' \quad (54)$$

and $\hat{f}_{\epsilon}(\underline{v}) = v_{\epsilon}(\underline{v})/v(\underline{v})$ (see formulae (30) and (31)), moreover we have,

$$d_{1,k,\underline{\alpha},0}(\underline{v}) = -e^{i k(\underline{x}_{\xi}(\underline{v}), \underline{\alpha})} [1 + \chi (n(\underline{x}_{\xi}(\underline{v})), \underline{\alpha})] \quad (55)$$

$$d_{2,k,\underline{\alpha},0}(\underline{v}) = -\nu(1+\chi) \frac{\lambda}{k} \hat{f}_{\epsilon}(\underline{v}) \cdot u_{G,\omega,\underline{\alpha}}^s(\underline{p} + \xi_{\epsilon}(v_1 + s(v_2)) \hat{\phi}(v_1) + \hat{z}(v_2)), \quad \underline{v} = (v_1, v_2)^T \in U, \quad (56)$$

and for $s = 1, 2, \dots$, we have,

$$d_{1,k,\underline{\alpha},s}(\underline{v}) = - \sum_{\nu=0}^{s-1} \frac{(\xi(\underline{v}) - \xi_r(\underline{v}))^{s-\nu}}{(s-\nu)!} \int_{U'} d\underline{v}' \cdot \left\{ \left[\left(\phi_k(\underline{v}), Q^{s-\nu}(\underline{v}, \underline{y}_{\xi_c}(\underline{v}')) \right) + \mathcal{L}^{s-\nu}(\underline{v}, \underline{y}_{\xi_c}(\underline{v}')) \right] \cdot c_{k,\underline{\alpha},\nu}(\underline{v}') + \frac{(1+\chi)}{\tilde{\zeta}k} \mathcal{L}^{s-\nu}(\underline{v}, \underline{y}_{\xi_c}(\underline{v}')) f_{k,\underline{\alpha},s}(\underline{v}') \right\} \quad \underline{v} \in U, \quad (57)$$

$$d_{2,k,\underline{\alpha},s}(\underline{v}) = -\mu \sum_{\nu=0}^{s-1} \frac{(\xi(\underline{v}) - \xi_r(\underline{v}))^{s-\nu}}{(s-\nu)!} \left\{ \left[\left(\phi_k(\underline{v}), Q^{s-\nu}(\underline{v}, \underline{y}_{\xi_c}(\underline{v}')) \right) + \mathcal{L}^{s-\nu}(\underline{v}, \underline{y}_{\xi_c}(\underline{v}')) \right] \cdot f_{k,\underline{\alpha},\nu}(\underline{v}') \right\}, \quad \underline{v} \in U. \quad (58)$$

Figure 2 shows an example of the relation between the sets Ω , Ω_r , Ω_c .

Roughly speaking assumptions (a_1) , (b_1) say that the spatial parts of the time harmonic components of the scattered field and of the auxiliary variable can be represented as single layer potentials generated by suitable densities defined on a surface $\partial\Omega_c$ contained in the interior of the smart obstacle $(\Omega; \chi)$. Assumptions (c_1) , (d_1) say that the smart obstacle is not far from being a more regular obstacle $(\Omega_r; \chi)$ and that the density functions of the single layer potentials of equations (48) and (49) can be expressed as a power series of the “distance” between the boundary of Ω and the boundary of Ω_r . Assumptions (a_1) , (b_1) make possible to formulate the boundary conditions (41), (42) as Fredholm integral equations of the first kind avoiding singular kernels even when $\partial\Omega$ is only Lipschitz continuous. These integral equations are ill posed so that to solve them numerically we try to take care of their ill-posedness using the perturbation series of equations (50) and (51) whose convergence is assumed in (c_1) , (d_1) . Note that thank to these last assumptions, we have reduced the solution of the optimal control problem to the solution of a set of systems of integral equations of the first kind whose ill-posedness is controlled via the perturbation approach.

Since we want to solve these systems of integral equations when the smart obstacle has complex geometry and the wavelength of the incoming wave is small compared to the characteristic dimension of the obstacle

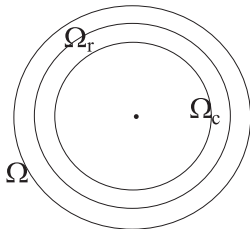


Fig. 2. An example of the relation between Ω , Ω_r , Ω_c .

we need to discretize the integral equations using finite dimensional vector spaces of high dimension. The use of suitable wavelet bases to represent the unknown densities, the data and the integral kernels of the integral equations (52) and (53) allows us to approximate the integral equations in finite-dimensional vector spaces of high dimension with sparse systems of linear equations that can be solved with affordable computing resources even when they involve hundreds of thousands or millions of unknowns and equations. This is due to the “sparsifying properties” of the wavelet basis used.

Let us introduce the wavelet basis used in the experiments of Section IV. Let $L^2(U')$ and $L^2(U)$ be the Hilbert spaces of square integrable real functions with respect to the Lebesgue measure defined on U' and on U respectively. As shown in [14], we generate a wavelet basis of $L^2(U')$ and of $L^2(U)$ using the tensor product and a suitable affine transformation of a wavelet basis of $L^2((0, 1))$. The wavelet basis of $L^2((0, 1))$ used in the numerical experiments presented in Section IV is generated via the multi-resolution analysis [18, 14] starting from the following orthonormal piecewise polynomial functions of $L^2((0, 1))$. Let us define three functions that are known as wavelet “mother” functions. Let $c_1 = 0.44721359549996$, $c_2 = 1.3416407864998$ and let V be the real matrix given by,

$$V = ((v_{i,j})_{i=1,2,3, j=1,2,3,4}) = \begin{pmatrix} 1 & -1 & -1 & 1 \\ -c_1 & c_2 & -c_2 & c_1 \\ -c_2 & -c_1 & c_1 & c_2 \end{pmatrix} \quad (59)$$

we define the following piecewise polynomial functions defined in the interval $(0, 1)$,

$$\Psi_i(z) = \begin{cases} v_{i,1}, & 0 < x < 1/4, \\ v_{i,2}, & 1/4 \leq x < 1/2, \\ v_{i,3}, & 1/2 \leq x < 3/4, \\ v_{i,4}, & 3/4 \leq x < 1, \end{cases} \quad i = 1, 2, 3, \quad (60)$$

and let $\psi_{i,m,\nu}(z)$, $z \in (0, 1)$, $i = 1, 2, 3$, $m = 0, 1, \dots$, $\nu = 0, 1, 2, \dots, 4^m - 1$ be the function defined by,

$$\psi_{i,m,\nu}(z) = \begin{cases} 4^{m/2} \psi_i(4^m z - \nu), & z \in (\nu 4^{-m}, (\nu+1) 4^{-m}), \\ 0, & z \in (0, 1) \setminus (\nu 4^{-m}, (\nu+1) 4^{-m}). \end{cases} \quad (61)$$

As shown in [14] the set $W_{a,b}$ defined as follows,

$$W_{a,b} = \left\{ \hat{\psi}_{j,m,\nu}(y) = \frac{1}{\sqrt{b-a}} \psi_{j,m,\nu} \left(\frac{y-a}{(b-a)} \right), y \in (a, b), \right. \\ \left. j = 1, 2, 3, m = 0, 1, \dots, \nu = 0, 1, 2, \dots, 4^m - 1 \right\} \\ \cup \left\{ L_0(y) = \frac{1}{\sqrt{b-a}}, y \in (a, b) \right\} \quad (62)$$

is an orthonormal basis of $L^2((a, b))$, $a < b$, $a, b \in \mathbf{R}$. We note that in equation (62) we have used the announced affine transformation to go from $L^2((0, 1))$ to $L^2((a, b))$ and that the wavelet mother functions Ψ_1 and Ψ_2 of $L^2((0, 1))$ defined in equation (60) have two vanishing

moments, that is: $\int_0^1 dx x^m \Psi_i(x) = 0$, $m = 0, 1$, $i = 1, 2$ while the wavelet mother function Ψ_3 of $L^2((0, 1))$ has only one vanishing moment, that is $\int_0^1 dx \Psi_3(x) = 0$ and we have $\int_0^1 dx x \Psi_3(x) \neq 0$.

Starting from this wavelet basis and using the tensor product the integral equations (52) and (53) can be reduced to a system of infinitely many linear equations whose unknowns are the coefficients of the representation on the wavelet basis of the density functions $c_{k,\underline{\alpha},s}$, $f_{k,\underline{\alpha},s}$, $s = 0, 1, \dots$. Truncating the wavelet expansions we reduce the approximate solution of the integral equations (52) and (53) to the solution of (eventually high dimensional) linear systems. These linear systems are approximated with sparse linear systems using a simple procedure that consists in setting to zero the elements of the matrices representing the integral kernels smaller in absolute value than a given threshold, in this way we obtain very sparse matrices. In fact, thank to the sparsifying properties of the wavelet basis introduced above, the kernels of the integral equations are approximated satisfactorily by the sparse matrices obtained with the procedure described above. Using these sparse matrices as coefficient matrices of linear systems that approximate those considered above we obtain sparse linear systems that approximate the integral equations (52) and (53). Finally, these sparse linear systems are solved with a suitable parallelization of the conjugate gradient method (see [16, 17]).

IV. NUMERICAL EXPERIENCE

In this Section we assume that the smart obstacle $(\Omega; \chi)$ and the ghost obstacle $(\Omega_G; \chi_G)$ have boundary acoustic impedance equal to infinity, i.e.: $\chi = \chi_G = +\infty$, that is the smart obstacle and the ghost obstacle are acoustically hard obstacles. This implies that the equations written in the previous Sections must be slightly changed to be adapted to deal with hard obstacles.

In the numerical experiments we consider as incoming acoustic fields time harmonic plane waves whose space dependent part is given by equation (46) or wave packets of the form,

$$u^i(\mathbf{x}, t) = e^{-[\underline{\gamma}, \mathbf{x}] - ct]^2 / 4\zeta^2}, \quad (\mathbf{x}, t) \in \mathbf{R}^3 \times \mathbf{R} \quad (63)$$

where $\underline{\gamma} \in \partial B$ and $\zeta \in \mathbf{R}$, $\zeta \neq 0$. The obstacle Ω in all the experiments is given by a smart simplified model of the NASA space shuttle. The original model of the NASA space shuttle (see Fig. 3(a)) has been modified obtaining the simplified NASA space shuttle (see Fig. 3(b)) in order to have an obstacle whose boundary can be represented with a single valued function in a suitable cylindrical coordinate system, that is in order to have the representation of equation (11) of the boundary of the obstacle for a suitable choice of the cylindrical coordinate system and of the function ξ . The data relative to the original obstacle (see Fig. 3(a)) are

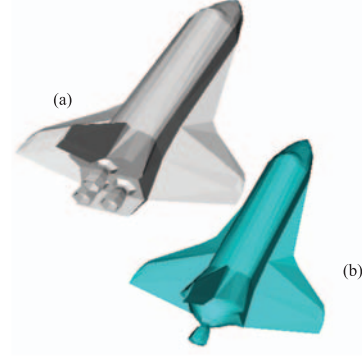


Fig. 3. (a) The NASA space shuttle, and (b) Simplified version of the NASA space shuttle.

available in the website <http://avalon.viewpoint.com/>. The physical dimensions of the shuttle are expressed in *units* where $1 \text{ unit} = 56.14/14 \text{ meters}$. The maximum length of the shuttle in the direction of the symmetry axis of its main body corresponds to 14 units . The space shuttle is an acoustically hard obstacle, this justifies the choice $\chi = +\infty$ made previously and the sound speed in the air at sea level is $331.45 \text{ meters/seconds}$ so that we choose $c = 331.45 \text{ meters/seconds}$ that corresponds to $c \simeq 82.65 \text{ units/seconds}$. Note that the z -axis of the cylindrical coordinate system used to represent the obstacle is chosen to be the “symmetry” axis of the main body of the simplified NASA space shuttle (see Fig. 4). In the following the lengths are expressed in *units*.

We choose $\underline{p} = (0, 7.5, 1.5)^T \in \mathbf{R}^3$, $z_i = z_i^G = -7$, $z_f = z_f^G = 7$, $z_i^* = -16$, $z_f^* = 16$, $s(z) = z_i^* + (z_f^* - z_i^*)(z - z_i)/(z_f - z_i)$, $z \in [z_i, z_f]$, $\xi_\epsilon(\phi, s(z)) = \sqrt{(1 - s(z)^2/d^2)/(\cos^2 \phi/a^2 + \sin^2 \phi/b^2)}$ where $a = 8$, $b = 13$, $d = 16$ and the ghost Ω_G is the translation of $\underline{p}_G = (0, 15, 2)^T \in \mathbf{R}^3$ of Ω . In Fig. 4 we show the setting of the ghost obstacle experiment studied here and the coordinate axes. The surfaces ξ_r , ξ_c have been chosen such that the kernels K_{ξ_r, ξ_c} and $\Phi(\mathbf{x}_{\xi_r}, \mathbf{y}_{\xi_c})$ defined in Section III are continuous with their first partial derivatives and we use always the first two terms of the operator expansion series given in formulae (50) and (51).

We remind that the website:

<http://www.econ.univpm.it/recchioni/scattering/w16> contains some auxiliary material that helps the understanding of the numerical experiments discussed here including stereographic and virtual reality applications.

The first experiment shows the effect due to the smart character of the obstacle for different incident time harmonic plane waves given in equation (46) and several values of the parameter λ , $0 \leq \lambda \leq 1$. We remind that we are assuming $\lambda \geq 0$, $\mu \geq 0$, $\mu + \lambda = 1$, $\varsigma = 1$ and that the smart obstacle reproduces exactly the field generated by the ghost obstacle on $\partial\Omega_\epsilon$ when $\mu = 0$,

$\lambda = 1$. The L^2 norm of the space dependent part of the pressure current $\tilde{\Psi}$ employed to obtain the ghost effect can be considered as a measure of the price paid in order to have the smart behaviour of the obstacle. We note that the quantity $n_{\psi,k}^\lambda$ defined in (equation (66)) is proportional to the L^2 norm of the space dependent part of the pressure current mentioned above.

Let us introduce the following quantities,

$$d_{s,G,\omega}^\lambda = \sqrt{\frac{\int_{\partial\Omega_\epsilon} |u_{\omega,\alpha}^s(\mathbf{x}) - u_{G,\omega,\alpha}^s(\mathbf{x})|^2 ds_{\partial\Omega_\epsilon}(\mathbf{x})}{\int_{\partial\Omega_\epsilon} |u_{G,\omega,\alpha}^s(\mathbf{x})|^2 ds_{\partial\Omega_\epsilon}(\mathbf{x})}} \quad (64)$$

$$d_{p,G,\omega} = \sqrt{\frac{\int_{\partial\Omega_\epsilon} |u_{p,\omega,\alpha}^s(\mathbf{x}) - u_{G,\omega,\alpha}^s(\mathbf{x})|^2 ds_{\partial\Omega_\epsilon}(\mathbf{x})}{\int_{\partial\Omega_\epsilon} |u_{G,\omega,\alpha}^s(\mathbf{x})|^2 ds_{\partial\Omega_\epsilon}(\mathbf{x})}}, \quad (65)$$

$$n_{\psi,\omega}^\lambda = \sqrt{\int_{\partial\Omega} |\varphi_{\omega,\alpha}(\mathbf{x})|^2 ds_{\partial\Omega}(\mathbf{x})}, \quad (66)$$

$$e_\omega^\lambda = \frac{d_{s,G,\omega}^\lambda}{d_{p,G,\omega}}, \quad (67)$$

where $u_{p,\omega,\alpha}^s$ is the field scattered by $(\Omega; \chi)$ as a passive obstacle, and $n_{\psi,\omega}^\lambda$, as said above, is the quantity that measures the ‘‘size’’ of the pressure current required to get the smart effect.

Table 1 shows the ghost effect obtained. In fact from left to right Table 1 shows the value of $\frac{\mu}{\lambda}$, ω/c , R_T , $d_{p,G,\omega}$, $d_{s,G,\omega}^\lambda$, e_ω^λ and $n_{\psi,\omega}^\lambda$, where R_T is defined as the ratio between the characteristic dimension of the obstacle and the wavelength of the incident time harmonic plane wave. The propagation direction of the incident plane wave in the coordinate system shown in Fig. 4 is $\underline{\alpha} = (\sin(\pi/4) \cos(\pi/4), \sin(\pi/4) \sin(\pi/4), \cos(\pi/4))^T$.

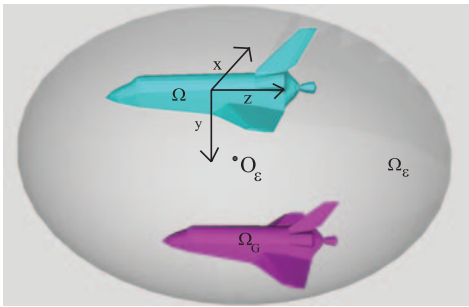


Fig. 4. The ghost obstacle experiment: the sets Ω (smart obstacle), Ω_G (ghost obstacle), Ω_ϵ (auxiliary set) and the coordinate system.

Note that when the ratio $\frac{\mu}{\lambda}$ goes to zero, i.e., when λ goes to 1, the ghost effect increases, in fact $d_{s,G,\omega}^\lambda$ decreases to zero and the price paid to obtain the ghost effect increases that is $n_{\psi,\omega}^\lambda$ increases. Moreover, the column e_ω^λ of Table 1 shows that when the wave number, $\frac{\omega}{c}$, increases the smart effect slightly deteriorates. In this experiment to solve the ghost obstacle scattering problem

Table 1. The ghost effect.

$\frac{\mu}{\lambda}$	$\frac{\omega}{c}$	R_T	$d_{p,G,\omega}$	$d_{s,G,\omega}^\lambda$	e_ω^λ	$n_{\psi,\omega}^\lambda$
0.1	10π	60	2.2791	0.5150	0.2259	31.632
0.001	10π	60	2.2791	1.872e-02	8.2112e-03	333.04
0.1	2π	14	0.5325	0.1003	0.1883	48.464
0.001	2π	14	0.5325	2.9671e-03	5.5718e-03	88.168
0.1	1	$\frac{7}{\pi}$	1.9351	0.2068	0.1068	28.290
0.001	1	$\frac{7}{\pi}$	1.9351	3.2942e-03	1.7036e-03	35.841

we have used 262144 real variables when $R_T = 60$, 16384 real variables when $R_T = 14$ and 1024 real variables when $R_T = 7/\pi$, that is we have solved linear systems of 262144, 16384, 1024 equations and unknowns when R_T is equal to 60, 14, $7/\pi$ respectively. The CPU time required to compute the field scattered by the smart obstacle when $R_T = 60$ is about 800 hours on the SP5 machine of the CASPUR center. This execution time includes the computation of the field scattered by the ghost obstacle as passive obstacle. Note that using a parallel implementation of the numerical code the clock time needed to compute the field scattered by the smart obstacle reduces to about six hours when we use 128 processors. We note that due to their condition number the linear systems used in this experiment must be solved with some care.

The second experiment shows the scattering from a time dependent incoming wave of equation (63) where $\underline{\gamma} = (\sin(\pi/4) \cos(\pi/4), \sin(\pi/4) \sin(\pi/4), \cos(\pi/2))^T$ (in the coordinate system of Fig. 4, and $\zeta = 1/(2\pi)$). In formulae (35), (36), (37), and (38) we have used the Gauss-Hermite quadrature rule with 400 nodes to approximate the Fourier transforms in the conjugate variable of time ω that give u^i , \tilde{u}^s , u_G^s , $\tilde{\varphi}$ respectively. Indeed with the choice $\zeta = 1/(2\pi)$ to get a satisfactory approximation of the incoming wave of equation (63) on an adequate compact set of the time axis only 30 wave numbers are needed. In order to compute the time harmonic components of the scattered waves of equations (36) and (37) we have used 1024, 4096, 16384 real variables to solve the time harmonic problems according with the value of R_T considered. We have chosen $\frac{\mu}{\lambda} = 10^{-10}$, $\mu = 1 - \lambda$, $\varsigma = 1$. We note that a rough estimate of the CPU time required to carry out this experiment is 5000 hours on the SP5 machine of the CASPUR center.

Let ∂D be the boundary of the sphere D having center in $O_\epsilon = O + \underline{p}$ (see Figs. 1 and 4) and radius 15.

Note that D contains Ω , Ω_G . Using the canonical spherical coordinate system (r, θ, ρ) we have,

$$\partial D = \{ \underline{x} = \underline{p} + (15 \sin \theta \cos \rho, 15 \sin \theta \sin \rho, 15 \cos \theta)^T \in \mathbf{R}^3, \theta \in [0, \pi], \rho \in [0, 2\pi) \}. \quad (68)$$

Figure 5 shows the field scattered by the passive obstacle $u_p^s(\mathbf{x}, t)$, by the smart obstacle $u^s(\mathbf{x}, t)$ and by

the ghost obstacle $u_G^s(\mathbf{x}, t)$ when $\mathbf{x} \in \partial D$, for three time values: $t = t_1 = -0.08, t_2 = 0.03, t_3 = 0.24$.

Figure 6 shows the value of the incoming field when $\mathbf{x} \in \partial D$ and $t = t_1, t = t_2, t = t_3$.

We note that in Fig. 5 the second and third columns are very similar, that is, the field scattered by the smart obstacle (second column) behaves as the field scattered by the ghost obstacle (third column). Furthermore, when the incoming acoustic field goes through D we can see that the passive and the ghost obstacle reacts in a different way when $t = t_1$ and $t = t_3$ and in a similar way when $t = t_2$. This effect is due to the fact that D is sphere with center in $O_\epsilon = O + \underline{p}$ that is in a point lying between the passive and ghost obstacles. So that, when $t = t_1$ the front of the incoming acoustic field (see Fig. 6 first column) is on the side where the passive obstacle is ($\phi \in [\pi/4, \pi]$) and when $t = t_3$ (see Fig. (6) third column) the incoming acoustic field is on the side where the ghost obstacle is ($\phi \in [3\pi/2, 2\pi]$).

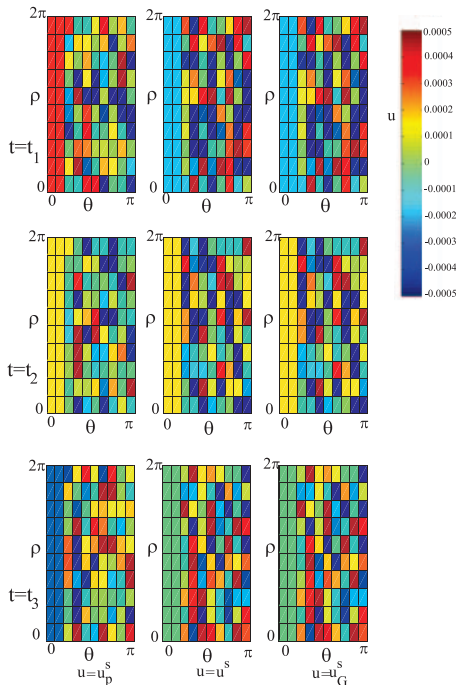


Fig. 5. The ghost effect on the surface of a sphere.

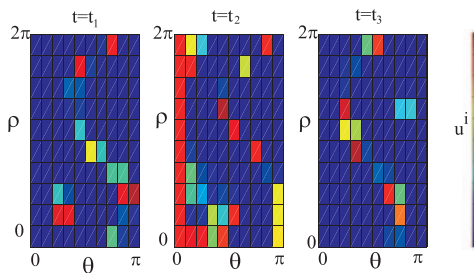


Fig. 6. The effect of the incoming field on the surface of a sphere.

ACKNOWLEDGEMENT

It is a pleasure to thank Mrs. Claudia Truini and Mr. Piero Lanucara of CASPUR (Roma, Italy) for the helpful assistance in the realization of the stereographic applications shown in the website associated with this paper.

REFERENCES

- [1] E. Mecocci, L. Misici, M. C. Recchioni, and F. Zirilli, "A new formalism for time dependent wave scattering from a bounded obstacle," *Journal of the Acoustical Society of America*, vol. 107, pp. 1825–1840, 2000.
- [2] F. Mariani, M. C. Recchioni, and F. Zirilli, "The use of the Pontryagin maximum principle in a furtivity problem in time-dependent acoustic obstacle scattering," *Waves in Random Media*, vol. 11, pp. 549-575, 2001.
- [3] L. Fatone, M. C. Recchioni, and F. Zirilli, "Some control problems for the Maxwell equations related to furtivity and masking problems in electromagnetic obstacle scattering," in *Mathematical and Numerical Aspects of Wave Propagation. Waves 2003*, G. C. Cohen, E. Heikkola, P. Joly, and P. Neittaanmaki Editors, Springer Verlag, Berlin, pp. 189-194, 2003.
- [4] L. Fatone, M. C. Recchioni, and F. Zirilli, "A masking problem in time dependent acoustic obstacle scattering," *Acoustics Research Letters Online*, vol. 5, no 2, pp. 25-30, 2004.
- [5] L. Fatone, M. C. Recchioni, and F. Zirilli, "Furtivity and masking problems in time dependent electromagnetic obstacle scattering," *Journal of Optimization Theory and Applications*, vol. 121, pp. 223-257, 2004.
- [6] L. Fatone, M. C. Recchioni, and F. Zirilli, "Mathematical models of "active" obstacles in acoustic scattering," in *Control and Boundary Analysis*, J. Cagnol and J. P. Zolesio Editors, Lecture Notes in Pure and Applied Mathematics, vol. 240, Marcel Dekker/CRC Press, Boca Raton, Fl. USA, pp. 119-129, 2005.
- [7] L. Fatone, G. Pacelli, M. C. Recchioni, and F. Zirilli, "Optimal control methods for two new classes of smart obstacles in time dependent acoustic scattering," *Journal of Engineering Mathematics*, vol. 56, pp. 385–413, 2006.
- [8] L. Fatone, M. C. Recchioni, A. Scoccia, and F. Zirilli, "Direct and inverse scattering problems involving smart obstacles," *Journal of Inverse and Ill-Posed Problems*, vol. 13, pp. 247-257, 2005.
- [9] L. Fatone, M. C. Recchioni, and F. Zirilli, "A method to solve an acoustic inverse scattering problem involving smart obstacles," *Waves in Random and Complex Media*, vol. 16, pp. 433-455, 2006.

- [10] L. Fatone, M. C. Recchioni, and F. Zirilli, “New scattering problems and numerical methods in acoustics,” in *Recent Research Developments in Acoustics*, S.G. Pandalai Managing Editor. Transworld Research Network, Kerala India, Vol. II, pp. 39-69, 2005.
- [11] L. Fatone, M. C. Recchioni, and F. Zirilli, “A numerical method to solve an acoustic inverse scattering problem involving ghost obstacles”, *Journal of Inverse and Ill-Posed Problems*, vol. 15, pp. 57–82, 2007.
- [12] D. Colton and R. Kress, *Integral Equation Methods in Scattering Theory*, John Wiley, New York, 1983.
- [13] L. Fatone, M. C. Recchioni, and F. Zirilli, “A numerical method for time dependent acoustic scattering problems involving smart obstacles and incoming waves of small wavelengths,” in *Mathematical Modeling of Wave Phenomena*, B. Nilsson, L. Fishman Editors, AIP Conference Proceedings, vol. 834, AIP Publ.,Melville, New York, pp. 109-121, 2006.
- [14] L. Fatone, M. C. Recchioni, and F. Zirilli, “New wavelet bases made of piecewise polynomial functions: approximation theory, quadrature rules and applications to kernel sparsification and image compression,” submitted to *SIAM Journal on Scientific Computing*.
- [15] J. Nečas, *Les Méthodes Directes en Théorie des Équations Elliptiques*. Masson & Cie. Publ., Paris, 1967.
- [16] M. C. Recchioni and F. Zirilli, “The use of wavelets in the operator expansion method for time dependent acoustic obstacle scattering,” *SIAM Journal on Scientific Computing*, vol. 25, pp. 1158–1186, 2003.
- [17] L. Fatone, G. Rao, M. C. Recchioni, and F. Zirilli, “High performance algorithms based on a new wavelet expansion for time dependent acoustic obstacle scattering,” *Communications in Computational Physics*, vol. 2, pp. 1139–1173, 2007.
- [18] S. Mallat, “Multiresolution approximation and wavelets”, *Transactions of the American Mathematical Society*, vol. 315, pp. 69–88, 1989.



nance.

Lorella Fatone Laurea in Mathematics cum Laude (1995), Ph. D. in Computational Mathematics and Operational Research, research fellow Universit di Modena and Reggio Emilia since 2001. Main research interests: numerical approximation of partial differential equations, mathematical finance.



tion, direct and inverse acoustic and electromagnetic scattering, mathematical finance.

Cristina Recchioni Laurea in Mathematics cum Laude (1987), associate professor of Mathematics at the Universit Politecnica delle Marche, Ancona since 2001. Author of over 60 scientific publications most of them published in international journals. Main research interests: numerical optimization, direct and inverse acoustic and electromagnetic scattering, mathematical finance.



and inverse acoustic and electromagnetic scattering, processing of remotely sensed data, mathematical finance.

Francesco Zirilli Laurea in Mathematics (1971), Laurea in Physics (1972), professor Universit di Roma “La Sapienza” since 1985. Author of over 150 scientific publications most of them published in international journals. Main research interests: partial differential equations, quantum field theory, nonlinear analysis, numerical optimization, direct and inverse acoustic and electromagnetic scattering, processing of remotely sensed data, mathematical finance.